THE CURRENT ROLE OF SAR INTERFEROMETRY FOR MAPPING AND FOREST BIOMASS ASSESSMENT IN THE BRAZILIAN AMAZON ENVIRONMENT

João R. Santos[1], Fabio F. Gama[1], Lênio S. Galvão[1], Camila Valéria J. Silva[1], Jose C. Mura[1]

1. National Institute for Space Research - INPE, SJC. Campos, Brazil; jroberto@dsr.inpe.br

ABSTRACT

This article presents the interferometric radar applications in the Brazilian tropical zones, through the analysis of two case studies: [1] the characterization of land cover using the interferometric coherence from Cosmo-SkyMed (X-band) images; [2] the aboveground biomass (AGB) estimates of succession chronosequence using the coherence from the TanDEM-X mission combined with the full polarimetric PALSAR/ALOS (L-band) attributes. In the first case, the study area is located in Humaitá region. Based on the Cosmo-SkyMed images, Himage mode, the interferometric coherence was generated. These data were classified by the Interacted Conditional Mode technique. Results showed an increase in the classification accuracy of 21% to separate the thematic classes (primary forest, wooded savanna, grass and shrub savanna, burned areas), using both the $\mathring{u}_{HH}$ and $ɔ_i$ attributes (kappa = 0.69). In the second case, the site was located in the Tapajós region. Multivariate regression was used to obtain the relationship between the interferometric coherence from TanDEM-X, combining the PALSAR full-polarimetric attributes, and the forest biomass content. The chronosequence in three stages of natural regrowth was established. Attributes like the ñvolumetric scatteringò (**P**v) from PALSAR and the interferometric coherence ($ɔ_i$) from TanDEM-X were important to explain the biomass content of this chronosequence ($R^2_{adjusted}$ = 0.75; RMSE = 28.78Mg.ha^{-1}), improving in 11% the model performance for the stock density prediction. The interferometric attribute from X-band showed a significant capability to improve the mapping and inventory of the forest landscape.

INTRODUCTION

Timely land cover information and biomass estimates are important for land resource conservation and management. The intense competition to produce different cash crops, sources of foods, biofuels and bioenergy and for ever-increasing urbanization (1), included new requirements to maintain and enhance the role of land as a carbon sink and to support biological diversity (2). Satellite remote sensing contributes to land use/land cover mapping and inventory due to its ability to obtain up-to-date detailed information over local and regional areas at low monitoring cost. Synthetic Aperture Radar (SAR) is an important alternative to optical remote sensing in tropical regions, providing additional information for land cover characterization.

Land cover studies using radar has become more practical since the launching of orbital SAR systems with regular data acquisition (3), such as the ERS 1/2 (C-band), Radarsat 1/2 (C-band), Envisat/ASAR (C-band), Cosmo-SkyMed (X-band), TerraSAR (X-band) and ALOS 1/2 - PALSAR (L-band). The physical principles of radar-interaction with the land cover components are complex. They determine the scattering mechanisms of the incident radiation that hits the target and returns to the radar sensor, whose response depends on the wavelength, polarization, and incidence angle of the imagery (4).

Several authors used SAR data for the discrimination of land cover, discussing the scattering mechanisms of the radar signals at different frequencies that interact with structural components of forest types. For instance, (5) used ERS-SAR tandem images for land cover mapping in African savannas by combining the interferometric coherence, average backscatter intensity and

backscatter intensity change images. (6) showed the potential of the backscattering and coherence images for land cover classification of tropical moist deciduous forest region (Karnataka, India) using ENVISAT/ASAR data. When analyzing ALOS-1/ PALSAR (L-band) and RADARSAT-2 (C-band) images, both in HH and HV polarizations, (7) compared the accuracy of the maximum likelihood, fuzzy ARTMAP and support vector machine classifiers for land-cover classification in the tropical moist region (Altamira region, Brazil). Multidate backscatter intensity and temporal coherence images (HH polarizations), derived from PALSAR/ALOS-1, were used by (8) to examine the improvement of land cover discrimination through maximum-likelihood classifier algorithm. Despite the existence of important studies to estimate forest biomass from radar imagery, there are very few examples in the literature that address the impact of spatial variability of forest structure (9) and its effect on biomass modeling. Some studies in the Brazilian Amazon using polarimetric and/or interferometric data were performed for this purpose by (10, 11, 12, 13, 14).

In this context, this work shows the results derived from two scientific studies in the Amazon region, as described below:

- the characterization of land use/land cover using the interferometric coherence from Cosmo-Skymed temporal images;
- the aboveground biomass (AGB) estimates of the successional chronosequence using the interferometric coherence from the TerraSAR-X/TanDEM mission combined with the full polarimetric PALSAR/ALOS (L-band) attributes.

STUDY AREA AND SAR DATA ACQUISITION

The first study was carried out in the Humaitá region (W 62° 58ô38" to 63° 22ô51" and S 7° 18ô30" to 7° 44ô38"), south of the Amazonas state. Two acquisitions (September 17-18, 2011) from Cosmo-SkyMed (X-band) images were made in the Stripmap mode - Himage, with HH polarization (5 m of resolution), ascendent pass and incidence angle of 26.7º. The vegetation of this area is constituted by Open Ombrophilous Forest with Savanna patches, where livestock and cash crops (rice, corn and soybeans) comprise the main economic activity. The second study was performed around the Tapajós region (NE Pará state), between the coordinates S $2^0$53ô12ò - $3^0$13ô20ò and W $54^0$53ô21ò - $55^0$04ô53ò The region is dominated by Dense and Open Ombrophilous Forests with land use associated to subsistence agriculture, large cash crops, cattle raising.

The ALOS-1/PALSAR images were acquired in the PLR 1.1 multipolarimetric mode (single look complex image), ascending orbit, with spatial resolution of 4.50 m in range and 9.50 m in azimuth. The incidence angle was 24°. By using the TanDEM-X (TerraSAR-X add-on for Digital Elevation Measurement) satellite with the almost identical twin-satellite TerraSAR-X, the first satellite-based single-pass SAR interferometer was formed. In this study, we used the interferometric data from 22 September 2011, with the following characteristics: stripmap mode, dual polarization (HH/HH), single look slant range complex, pixel resolution of 1.42 m (range) and 2.54 m (azimuth). In both studies, the field campaigns for identification of the thematic classes (Humaitá site) and for forest inventory (Tapajós site) were performed simultaneously to SAR data imagery.

THE INSAR COHERENCE FOR LAND COVER MAPPING FROM COSMO-SKYMED

Here, an attempt is made to demonstrate the potential of SAR interferometry (InSAR) for land-cover mapping by exploiting the sensitivity of coherence for various land-cover features. From two Cosmo-SkyMed images with 1 day of revisit time, the InSAR-derived interferometric coherence (ɔi,) was obtained. This attribute represents the modulus of the correlation coefficient between them and is calculated through the equation:

$$\left| \rho_{ji} \right| = \frac{|\langle S_1 S_2^* \rangle|}{\sqrt{\langle |S_1|^2 \rangle \langle |S_2|^2 \rangle}} \quad \text{(Eq.1)}$$

where ɟ ɔi = complex correlation coefficient; S_1 and S_2 represent the master and slave complex co-registered images; < > gives the expectation value, and * denotes the complex conjugate.

The coherence varies between 0 (incoherence) and 1 (perfect coherence) and is a function of the systemic spatial decorrelation, additive noise, and scene decorrelation that takes place between the two acquisitions.

The mapping of land cover in this work was conducted by a contextual Markovian classification technique known as Iterated Conditional Modes-ICM (15). The contextual classification begins with a standard maximum likelihood classification map (with equal a priori probabilities) using the same training areas that ICM uses. The ICM algorithm runs until the changes from one interaction to another fall below a threshold established by the user; in this case, this threshold was set at 5%. Expressing the strength (or intensity) of radar signals received by the sensor after scattering, the backscattering coefficient is a fundamental indicator of ground conditions, particularly of vegetation growth, due to its sensitivity to surface roughness with respect to polarization (4). Therefore, we first applied the ICM classification over the backscatter (ů°$_{HH}$) image and later over an integrated product composed of the backscatter + interferometric coherence + coherence/backscatter (ɔ$_i$ / ů°$_{HH}$) ratio. The inclusion of the coherence parameter in this triplet of images (Figure 1) allowed an increase of 21% in classification accuracy (Kappa = 0.69), compared to the accuracy resultant from the use solely of backscatter image (Kappa = 0.546).

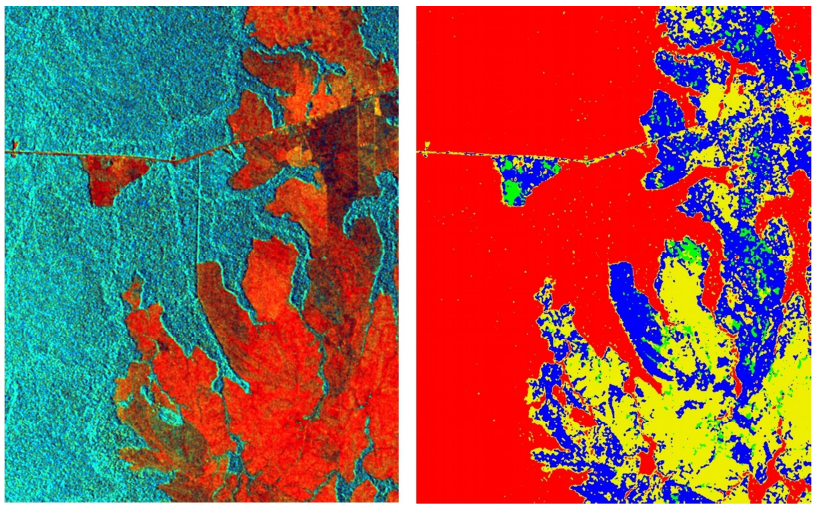

Classes	PF	B	WS	GSA	Row Σ
PF	29942	0	5	23	29970
B	0	191	103	230	524
WS	0	53	1305	1166	2524
GSA	42	7	1776	1417	3242
Col. Σ	29984	251	3189	2836	36260

Kappa =	0.69	Overall Acuracy (%) =	90.61
Tau =	0.87	Overall Error (%) =	9.39

Figure 1. (a) Color composite image combining the InSAr coherence(red) + backscatter (green) + ratio of coherence/backscatter (blue) derived from Cosmo-SkyMed (Stripmap mode); (b) ICM land cover classification with Primary Forest(PF) in red, Burned area (B) in green, Wooded Savanna (WS) in blue; Grass/shrub Savanna Area(GSA) in yellow; (c) the classification performance matrix.

The inclusion improved the discrimination of complex classes such as primary forest, wooded savanna, grass and shrub savanna and burned areas, located in the transition zone between the two forest ecosystems. In relation to the spatial feature attributes, the primary forest presented interferometric coherence values of 0.1489 (± 0.0544), which increased to 0.4039 (± 0.1116) and 0.4513 (± 0.091) for wooded savanna and grass/shrub savanna, respectively

THE INSAR COHERENCE FOR BIOMASS MODELING OF TROPICAL SUCCESSION CHRONOSEQUENCE FROM TANDEM-X COMBINED TO FULL-POLARIMETRIC PALSAR

In this study, we discuss the capability of the full polarimetric PALSAR (L-band) attributes, when combined with the interferometric coherence (**ɔ$_i$**) from the TerraSAR/TanDEM mission (X-band), to characterize the different stages of secondary succession and to improve the AGB estimates of the successional chronosequence located in the Brazilian Tapajós region.

Initially, polarimetric and radiometric calibrations and a resampling procedure (*multi-look*) in the PALSAR images were performed, followed by the application of the modified Lee filter (window of 5 x 5 pixels). After that, the backscatter (ů°) of each polarization was obtained. Then, the conversion procedure of complex scattering matrix [S] into covariance [C] and coherence [T] matrices was made, from which attributes comprising different polarimetric characteristics for each regrowth vegetation type were calculated. The following radar attributes, which are based on information from the real part of each pixel, were considered: backscatter coefficient (ů°); the ratio of parallel polarization (Rp) and cross polarization (Rc); the indices, formulated by (16), referred to biomass index (BMI), canopy structure index (CSI) and volume scattering index (VSI); and also the radar forest degradation index (RDFI) proposed by (9). Others attributes that take advantage of the SAR phase information were also evaluated: the polarimetric coherence of HH-VV (**ɔ**) and phase difference of HH-VV (**ɸ**); parameters resulting from the target decomposition (17) by the coherence matrix [T], named entropy (H), anisotropy (A) and the mean alpha angle ($\bar{\alpha}$) ; the volume scattering components (*Pv*), double bounce (Pd) and surface (Ps), resulting from the [C] decomposition matrix (18); the magnitude (Ůs) and Touzi phase (∧Ůs) as well as the orientation angle (**ɣ**) and helicity ($\acute{U}_h$), also derived from the same former decomposition (19). On its turn, from the TanDEM-X data, the interferometric coherence ($ɔ_i$,) was obtained from Equation 1.

All these attributes from both radar sensors were extracted in regions of interest (ROIs) representing each thematic class, corresponding to the each plot properly georeferenced and inventoried in the field survey. During the survey, we measured the dendrometric parameters of trees (DBH and total height) that served to model the biomass through the allometric equations. In order to represent the structural variability of the successional chronosequence in the Tapajós site, face to their radar response, 25 plots with a total sampled area of 5.5 ha were inventoried.

Multiple regression analysis was employed to examine the sensitivity of the PALSAR attributes and the interferometric coherence from TanDEM-X to model the forest biomass trajectory. This regression model was adjusted using Ordinary Least Squares (OLS). The previous selection of explanatory variables, based on the inspection of the correlation matrix, was carried out using also the ñbest subsetò procedure. The model performances were verified from the analysis of R^2, $R^2_{adjusted}$, RMSE and Cp Mallow criteria, as well as the diagnosis of multi-colinearity (by calculation of Variance Inflation Factor ï VIF), analysis of outliers (Cook´s distance) and residuals. Then, we validated the best model using a hold-out set of samples.

In the preliminary analysis of the successional chronosequence structure, we observed that the initial regrowth presented an aboveground biomass of 14.59 ± 4.37 (ton.ha^{-1}). The intermediate and advanced regrowth had 56.34 ± 3.77 and 107.50 ± 5.82 ton.ha^{-1}, respectively. It is important to mention that primary forests, also inventoried in this Tapajós site, had aboveground biomass of 340.56 ± 10.22 ton.ha^{-1}. This fact demonstrates that there is still a long time for resetting the chronological trajectories of carbon content, reflecting the fragmentation level of the landscape, the edaphic conditions, in addition to the differences in earlier land use.

Based on the series of statistical parameters, which included R^2, $R^2_{adjusted}$, RMSE, Cp Mallow and Variance Inflation Factor, and combining the interferometric coherence ($ɔ_i$) from TanDEM-X and PALSAR (L-band) attributes, the best regression biomass model (Figure 2) presented R^2 of 0.78 and R^2adj value of 0.75. It was expressed by:

$$\textbf{log AGB} = \textbf{2.963} - \textbf{2.5359} * ɔ_i + \textbf{5.26954} * \textbf{Pv} \qquad \text{(Eq. 2)}$$

where: log AGB is the logarithmic mode of biomass; $ɔ_i$ is the interferometric coherence*;* and *Pv,* is the volumetric scattering derived from Freeman-Durden target decomposition model.

The variable $ɔ_i$ is more sensitive to the arboreal components. The density and arrangement in the strata of each succession stage (one stratum in the young phase; two or three strata, according to the oldest regeneration period) are perceived differently by the radar with different frequencies and imaging modes, when the responses of forest typologies are expressed as biomass. In a more detailed analysis of the regression models, one concluded that the volumetric scattering, among all

PALSAR (L-band) attributes, had the highest incremental predictive power. However, after adding the interferometric coherence from TanDEM-X, the stock density prediction of the model improved by 11 % for the secondary succession stands.

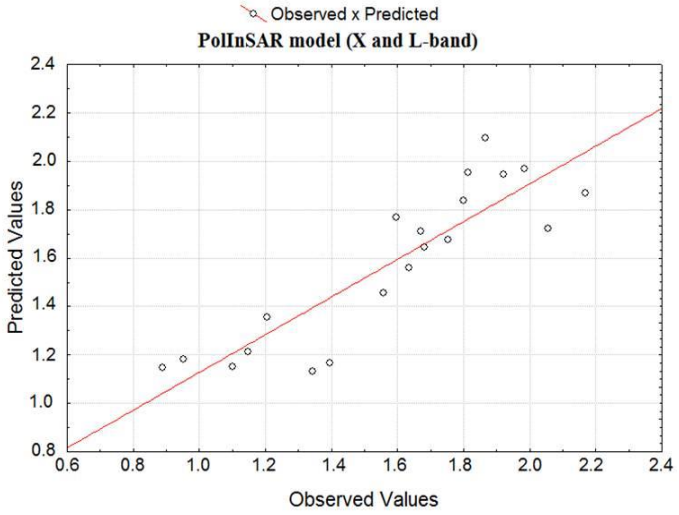

Figure 2. Estimated vs. ground-observed biomass (in log) of secondary succession for PALSAR combined with TanDEM dataset.

CONCLUSIONS

Based on the two scientific works, we concluded that:

- The thematic performance was improved using Cosmo-SkyMed images, through the ICM classifier, when the coherence was included as an input variable;

- The combination of interferometric coherence and polarimetric attributes (from X- of TanDEM and L- bands of PALSAR) improved the AGB estimates, especially because they are sensitive to variations in the vertical structure of forest typology. This occurs mainly in successional trajectories, which present lower biomass values compared to the mature forest.

ACKNOWLEDGEMENTS

The authors are grateful to the Brazilian institutions CAPES and CNPq for the fellowhsips; the MPEG for the botanical assistance; the LBA-Santarém Office for the logistic support during the field survey; and ICMBio/MMA - Sisbio Process 35010-1 and 38157-2). Thanks also to the JPL and CALTEC/USA (under a contract with NASA ï task number 281945.02.61.02.82) and DLR/Germany for processing and delivery of the TanDEM-X data.

REFERENCES

1 De Castro P, F Adinolfi, F Capitanio, S Di Falco, A Di Mambro (Eds.), 2013. The Politics of Land and Food Scarcity, Routledge (Abingdon, UK), 154 pp.

2 Mollicone D, F Achard, S Federici, H D Eva, G Grassi, A Belward, F Raes, G Seufert, H J Stibig, G McKenney, B A, J M Kiesecker, 2010. Policy development for biodiversity offsets: a review of offset frameworks. Environment Management, 45 (1): 165ï 176.

3 Jin H, G Mountrakis, S V Stehman, 2014. Assessing integration of intensity, polarimetric scattering, interferometric coherence and spatial texture metrics in PALSAR-derived land cover classification. ISPRS Journal of Photogrammetry and Remote Sensing, 98: 70ï 84.

4 Koch B, 2010. Status and future of laser scanning, synthetic aperture radar and hyperspectral remote sensing data for forest biomass assessment. ISPRS Journal of Photogrammetry and Remote Sensing, 65: 581-590.

5 Okhimamhe A A, 2003. ERS SAR interferomeytry for land cover mapping in a savanna area in Africa. International Journal of Remote Sensing, 24(18): 3583-3594.

6 Nizalapur V, 2008. Land cover classification using multi-source data fusion of ENVISAT-ASAR and IRS P6 LISS-III Satellite dat - a case study over tropical moist deciduous forested regions of Karnataka, India. In: International Archives of Photogrammetry, Remote Sensing and Spatial Information on Sciences. v. XXXVII, Part B6b, Beijing, 329-332.

7 Li G, L Dengsheng, E Moran, L V Dutra, M Batistella, 2012. A comparative analysis of ALOS PALSAR L-band and RADARSAT-2 C-band data for land-cover classification in a tropical moist region. ISPRS Journal of Photogrammetry and Remote Sensing, 70: 26ï 38.

8 Parihar N, A Das, V S Rathore, M S Nathawat, S Mohan, 2014. Analysis of L-band SAR backscatter and coherence for delineation of land-use/land cover. International Journal of Remote Sensing, 35(18): 6781-6798.

9 Saatchi S, M Marlier, R L Chazdon, D B Clark, A E Russel, 2011. Impact of spatial variability of tropícal forest structure on radar estimation of aboveground biomass. Remote Sensing of Environment, 115: 2836-2849.

10 Neeff T, G S Biging, L V Dutra, C C Freitas, J R Santos, 2005. Modeling spatial tree pattern in the Tapajós forest using interferometric height. Revista Brasileira de Cartografia, 57(1): 1-6.

11 Santos J R, I S Narvaes, P M L A Graça, F G Gonçalves, 2009. Polarimetric responses and scattering mechanisms of tropical forests in the Brazilian Amazon. In: Advances on Geoscience and Remote Sensing. (Org.) Gary Jedlovec (NASA/ MSFC-USA), 1ed., v. 8, Vukovar,Croatia: IN-TECH, 183-206.

12 Treuhaft R N, F G Gonçalves, J B Drake, B D Chapman, J R Santos, L V Dutra, P M L A Graça, G H Purcell, 2010. Biomass estimation in a tropical wet forest using Fourier transforms of profiles from lidar or interferometric SAR. Geophysical Research Letters, 37: L23403.

13 Bispo P C, J R Santos, M M Valeriano, R Touzi, F M Seifert, 2014. Integration of polarimetric PALSAR attributes and local geomorphometric variables derived from SRTM for forest biomass modeling in Central Amazonia. Canadian Journal of Remote Sensing, 40: 26-42.

14 Treuhaft R.; F G Gonçalves, J R Santos, M M Keller, M Palace, S Madsen, F Sullivan, P M L. A Graça, 2015. Tropical-forest biomass estimation at X-Band from the spaceborne TanDEM-X interferometer. IEEE Geoscience and Remote Sensing Letters (Print), 12: 239-243.

15 Freitas C C, L S Soler, S J S Santâanna, L V Dutra, J R Santos, J C Mura, A H Correia, 2008. Land Use and Land Cover Mapping in the Brazilian Amazon Using Polarimetric Airborne P-Band SAR Data. IEEE Transactions on Geoscience and Remote Sensing, 46 (10): 2956-2970.

16 Pope K O, J M Benayas-Rey, J F Paris, 1994. Radar remote sensing of forest and wetland ecosystems in the Central American tropics. Remote Sensing of Environment, 48(2): 205-219.

17 Cloude S R, E Pottier, 1996. A review of target decomposition theorems in radar polarimetry. IEEE Transactions on Geoscience and Remote Sensing., 34(2): 498-518.

18 Freeman A, S L Durden, 1998. A three-component scattering model for polarimetric SAR data. IEEE Transactions on Geoscience and Remote Sensing, 36(3): 963-973.

19 Touzi R, 2007. Target scattering decomposition in terms of roll-invariant target parameters. IEEE Transactions on . Geoscience and Remote Sensing, 45(1): 73-84.